14th Australasian Fluid Mechanics Conference
Adelaide University, Adelaide, Australia
10-14 December 2001

Pressure Fluctuations on Cylinders with Thick Turbulent Boundary Layers in Axial and Near-Axial Flow

F. L. Berera and M. K. Bull

Department of Mechanical Engineering
University of Adelaide, Adelaide, South Australia, 5005 AUSTRALIA

Abstract

Results are presented of an investigation of surface-pressure fluctuations beneath turbulent boundary layers, with thicknesses up to 11 times the cylinder radius, on cylinders in axial and near-axial flow. Attention is concentrated on the power spectrum of the surface-pressure field. The investigation ranges over axial flow; flows with small angles of yaw (up to 1°), which produce distorted but still-recognisable boundary layers; and flows at yaw angles (up to 9°) sufficiently large for the boundary-layer flow to give way to oblique vortex shedding from the cylinder. It is concluded that the spectra of axisymmetric boundary layers are consistent with the distinct frequency regimes which characterise the spectra of planar boundary layers, but that the low-frequency regime may be more extensive; and that, despite the gross asymmetries in the outer regions of the boundary layer produced by small yaw angles, the scale of the main pressure-producing region of the layer changes very little with yaw angle.

Introduction

In the present paper, attention is concentrated on the power spectrum of the surface-pressure fluctuations beneath the turbulent boundary layer developed on a long cylinder. The effects on the spectrum of increasing surface curvature (characterised by the cylinder radius a) in axisymmetric flow, and of yawing the cylinder axis to the oncoming stream, are examined.

A long history of measurement of surface-pressure fluctuations associated with turbulent boundary layers on flat plates shows that, as a reflection of the fact that multiple scales are required to describe the structure of the boundary layer itself, the power spectral density of the pressure, $\varphi_p(\omega)$, does not scale with either inner-layer or outer-layer boundary-layer parameters in any simple way. Experimental results suggest that (Bull, [2]) four ranges of frequency can be identified in which the spectral scaling takes different forms:

1. Low-frequency range:
   $\omega\delta^*/U_0 \leq 0.03$, $\varphi_p(\omega)U_0/q^2\delta^* = k_1\,(\omega\delta^*/U_0)^2$;
2. Mid-frequency range:
   $5 \leq \omega\delta/u_\tau \leq 100$, $\varphi_p(\omega)u_\tau/\tau_w^2\delta = f_2\,(\omega\delta/u_\tau)$;
3. Universal range:
   $100 \leq \omega\delta/u_\tau \leq 0.3\delta^+$, $\omega\varphi_p(\omega)/\tau_w^2 = k_3$;
4. High-frequency range:
   $\omega\nu/u_\tau^2 \geq 0.3$, $\varphi_p(\omega)u_\tau^2/\tau_w^2\nu = f_4\left(\omega\nu/u_\tau^2\right)$,

where U_0 is the flow speed, δ and δ^* the thickness and displacement thickness of the boundary layer, τ_w the wall shear stress, $u_\tau = \sqrt{\tau_w/\rho}$, ρ and ν the density and kinematic viscosity of the fluid, $q = (1/2)\rho U_0^2$, $\delta^+ = \delta u_\tau/\nu$, k_1 and k_3 are constants, and f_2 and f_4 represent functions. These flat-plate relations are used as a reference for comparison with the experimental data obtained in the present work.

Experimental Arrangements

The measurements were made in a recirculating water-channel, with a working section 176 mm wide, 400 mm deep and 3 m long. Water flows to the test section via a settling chamber, honeycomb, screens, and a 4:1 contraction. Flow rate is controlled by an adjustable weir at the downstream end of the test section. The test section is mechanically decoupled from the rest of the circuit, and very effectively vibration-isolated; background acoustic noise in it is thereby minimised.

The experimental models were circular cylinders, 6.35 mm in diameter, composed of an upstream segment of acrylic tube, variable in length from 0.3 m to 2.7 m, and a downstream segment fitted with pressure transducers and accelerometers. The pressure sensors were connected to the cylinder surface by water-filled pin-holes of diameter $d = 0.4$ mm.

Pressure-fluctuations were measured on cylinders of various lengths in axial flow. Thereby, turbulent boundary layers with thicknesses in the range $3.2 \leq \delta/a \leq 11.5$, at distances x downstream of the origin of the boundary layer in the range $94 \leq x/a \leq 850$, could be investigated. The flow speed was $U_0 \simeq 1.2$ m/s in all cases, and the cylinder Reynolds number therefore essentially constant at $Re_a = aU_0/\nu \simeq 3.3 \times 10^3$.

In a second series of experiments, a cylinder about 1.8 m long was inclined at various yaw angles to the mean flow direction. The wall-pressure fluctuations were measured at three circumferential positions at a fixed downstream position, $x/a = 491$, at azimuthal angles $\theta = 0°$, 90° and 180° measured from the leeward side of the yawed cylinder.

The flow parameters for the two series of experiments are given in table 1 and 2.

x/a	δ/a	δ/δ^*	θ/δ^*	Re_θ	C_f
94	3.2	7.38	1.23	1.2×10^3	5.69×10^{-3}
164	4.8	7.14	1.19	1.8×10^3	5.08×10^{-3}
283	6.6	6.95	1.14	2.9×10^3	4.81×10^{-3}
491	9.4	6.85	1.11	4.1×10^3	4.69×10^{-3}
850	11.5	6.86	1.08	5.0×10^3	4.64×10^{-3}

Table 1: Boundary layer characteristics – Cylinders in axial flow.

Effects of Transducer Resolution

Schewe [6] concluded that a pressure transducer with

$\beta[^\circ]$	x/a	$\delta_{\theta=180^\circ}/a$	$\delta_{\theta=180^\circ}/\delta_{\theta=0^\circ}$
0.0	491	9.4	1.05
0.2	491	5.9	0.67
0.4	491	5.5	0.50
0.6	491	3.7	0.29
0.8	491	3.3	0.18
1.0	491	2.5	0.09
3.0	491	-	-
9.0	283	-	-

Table 2: Boundary layer characteristics – Yawed cylinders.

$d^+ = du_\tau/\nu \simeq 20$ is sufficiently small to resolve the wall-pressure-fluctuation spectrum over its entire frequency range; and for the pinhole in the present work, $d^+ \simeq 20$. For adequate resolution, the transducer must be small in relation to a wavelength of any particular turbulence component, of frequency ω, convected at velocity U_c; this implies $d^+ \ll 2\pi(U_c/U_0)U_0^+/\omega^+$, where $\omega^+ = \omega\nu/u_\tau^2$. With U_c/U_0 as low as 0.5 for high frequency components, $U_0^+ \simeq 20$ and $d^+ \simeq 20$, this is equivalent to a frequency limitation of $\omega^+ < 3$. Since the present measurements are limited to $\omega^+ < 1.5$, serious resolution errors are unlikely. However, the presence of the pinhole itself can lead to over-estimation of the power spectral density at frequencies exceeding a value as low as $\omega^+ = 0.1$ (Bull and Thomas, [4]). The present data would be subject to such errors, and, to avoid inconsistencies as far as possible, the flat-plate data obtained from pinhole measurements (with somewhat higher d^+) by Farabee and Casarella [5] are used for comparisons of flat-plate and cylinder spectra.

Wall-Pressure Power Spectra for Axial Flow, $\beta = 0$

Dimensional spectra of the surface-pressure fluctuations on the cylinder in axial flow are shown in figure 1, for a range of values, $3.2 \leq \delta/a \leq 11.5$, of the ratio of boundary layer thickness to cylinder radius. Increasing

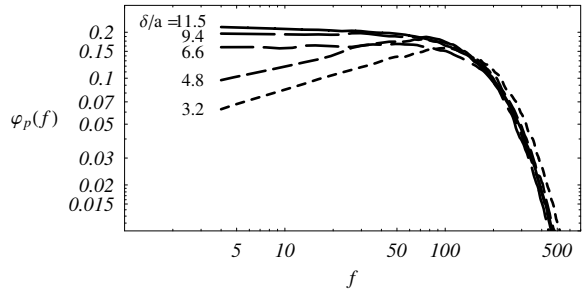

Figure 1: Power spectral density of wall-pressure fluctuations on a cylinder in axial flow as a function of frequency for various values of δ/a.

δ/a brings about a shift of spectral energy from high to low frequency. The increase in spectral level at low frequencies closely balances the decrease at high frequencies, so that the overall mean-square pressure $\overline{p^2}$ is essentially independent of δ/a over the experimental range. The ratio of root-mean-square pressure to dynamic pressure is $p_{rms}/q = 9.5 \times 10^{-3}$, which is similar to the flat-plate values of $p_{rms}/q = 9.65 \times 10^{-3}$ obtained by Farabee and Casarella [5] with pinhole sensors and $p_{rms}/q = 9.8 \times 10^{-3}$ found by Schewe [6] using miniature flush-mounted sensors.

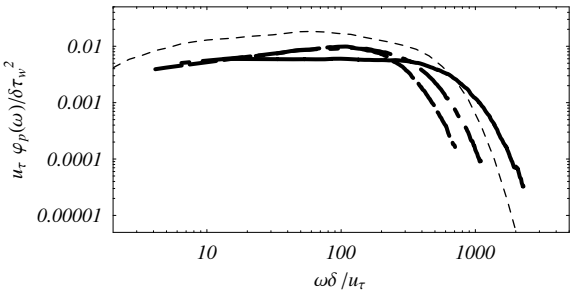

Figure 2: Non-dimensional power spectral density of wall-pressure fluctuations in axial flow scaled on mid-frequency form. ------: Farabee and Casarella [5]; ——: $\delta/a = 3.2$; —·—: $\delta/a = 4.8$; ——: $\delta/a = 9.4$.

Scaling of the data in the non-dimensional form appropriate to the flat-plate mid-frequency range, namely $\varphi(\omega)u_\tau/\tau_w^2\delta$ as a function of $\omega\delta/u_\tau$, (figure 2) produces a good collapse over a range of non-dimensional frequencies $5 \leq \omega\delta/u_\tau \leq 50$. However, the collapsed data are not in very close agreement with a typical flat-plate spectrum of [5] in the same frequency range.

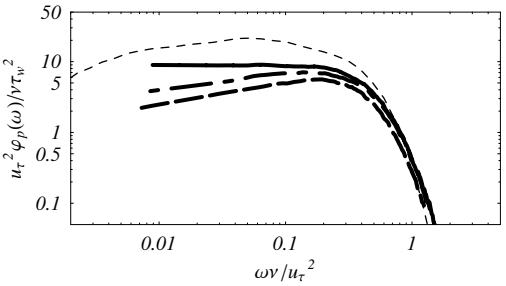

Figure 3: Non-dimensional power spectral density of wall-pressure fluctuations in axial flow scaled on high-frequency form (see figure 2 for caption).

The present data are rescaled in the form of the flat-plate high-frequency range, that is as $\varphi(\omega)u_\tau^2/\tau_w^2\nu$ as a function of $\omega\nu/u_\tau^2$, in figure 3. All the spectra now collapse onto a single curve, almost identical to that for the flat-plate layer, for non-dimensional frequencies $\omega\nu/u_\tau^2 \geq 0.3$.

Wall-Pressure Power Spectra for Very Small Yaw Angles, $0^\circ \leq \beta \leq 1^\circ$

Dimensional pressure spectra obtained for yaw angles $\beta = 0^\circ, 0.6^\circ$ and 1° are shown in figure 4. Yaw-angle postscripts L and W denote the leeward ($\theta = 0^\circ$) and windward side ($\theta = 180^\circ$) of the cylinder. The spectral levels on the windward side are essentially constant and independent of yaw angle for frequencies below 100 Hz, but at higher frequencies, $f \geq 100$ Hz, increase with the yaw angle. On the leeward side, however, the levels appear to decrease uniformly over the whole frequency range as the yaw angle is increased. The power spectra at $\theta = 90^\circ$ (not shown) retain their $\beta = 0^\circ$ values at all yaw angles smaller than 1°.

As indicated in table 2, very small angles of yaw have a quite profound effect on the symmetry of the boundary layer, thinning it on the windward side of the cylinder and thickening it on the leeward side: even for $\beta = 1^\circ$, the thickness of the layer on the leeward side is more than ten times that on the windward side. For the same

yaw angle of $\beta = 1°$, the spectral levels at low frequencies are about 1.5 times greater on the windward than on the leeward side. In this case, similarity of the windward and leeward spectra, by mid-frequency flat-plate scaling on local variables, would require the wall shear stress to be greater on the windward than the leeward side by an unlikely factor of about 6.5: the only available (indirect) evidence, from the experiments of Bücker and Lueptow [1], indicates that no dramatic change in wall stress occurs at such small angles of yaw. This implies that flat-plate mid-frequency scaling on local variables is inappropriate for yawed cylinders.

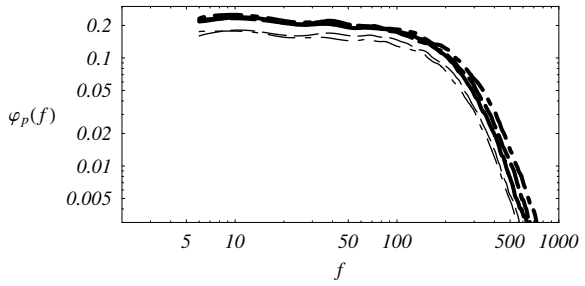

Figure 4: Power spectral density of wall-pressure fluctuations for slightly yawed cylinders, $\beta \leq 1°$. —·—: $\beta = 1°L$; – – – –: $\beta = 0.6°L$; ——: $\beta = 0°$; — —: $\beta = 0.6°W$; — · —: $\beta = 1°W$.

With increasing yaw angle, the root-mean-square pressure fluctuation shows an increase on the windward side of the cylinder, a slightly more pronounced decrease on the leeward side, and scarcely any change at $\theta = 90°$.

The present experimental results, for yaw angles $\beta \leq 1°$ are in large part in agreement with earlier measurements made on a 1-inch-diameter cylinder by Willmarth et al. [7] for a single yaw angle of $\beta = 2.36°$. However, when the smaller cylinder used here was investigated at a similar yaw angle (3°), a significantly different form of wall-pressure power spectrum was observed; this is discussed in the next section.

Wall-Pressure Power Spectra for Larger Yaw Angles, $1° \leq \beta \leq 9°$

Power spectra, again dimensional, for yaw angles up to 9° are shown in figure 5. The most striking result, referred

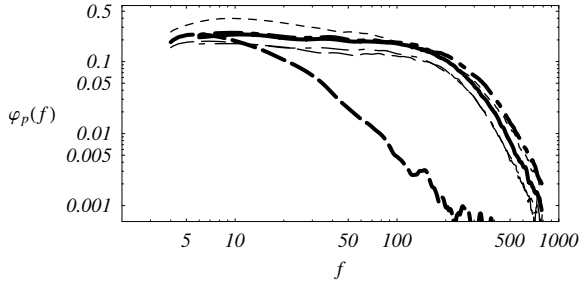

Figure 5: Power spectral density of wall-pressure fluctuations for yawed cylinders, $1° \leq \beta \leq 9°$. – – – – –: $\beta = 9°L$; – – – –: $\beta = 3°L$; —·—: $\beta = 1°L$; ——: $\beta = 0°$; — · —: $\beta = 1°$; — —: $\beta = 3°$.

to in the previous section, is the dramatically reduced spectral levels on the windward side of the cylinder for $\beta = 3°$. On the opposite side of the cylinder, the spectrum still has the same form as all the windward and leeward spectra at smaller yaw angles, $0° \leq \beta \leq 1°$. For $\beta = 9°$, the spectrum on the windward side (not shown) also exhibits greatly reduced levels and is nearly identical to that for $\beta = 3°$. In contrast, elevated spectral levels occur on the leeward side at low frequencies, but with little change at high frequency.

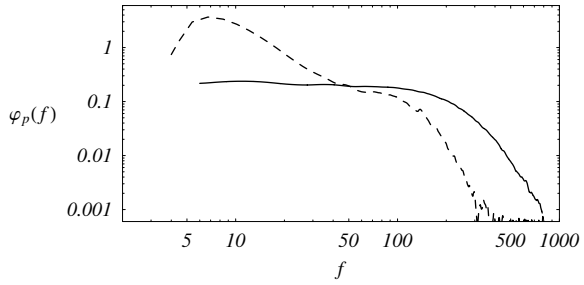

Figure 6: Power spectral density of the wall-pressure fluctuations on a yawed cylinder ($\beta = 9°$) measured at an azimuthal angle of $\theta = 90°$ from the windward side. ——: $\beta = 0°$; – – – – –: $\beta = 9°$.

The power spectrum measured at $\theta = 90°$ for $\beta = 9°$ (figure 6) exhibits new features, namely a broad spectral peak at a frequency of about 6 Hz and a substantial drop in the spectral levels, relative to those for axial flow, for frequencies greater than 60 Hz. The effect appears to result from eddy shedding from the yawed cylinder. The investigation of Bull and Dekkers [3] indicates that vortex shedding would occur under these flow conditions, but at a somewhat higher frequency. The difference is apparently due to control of the frequency by cylinder vibration (confirmed by acceleration spectra). Even so, this spectrum perhaps indicates the nature of spectral changes to be expected from natural vortex shedding.

Discussion

The wall-pressure spectrum is a summation of effects of turbulence in all parts of the boundary layer, and therefore derives contributions from pressure-producing eddies of various scales. In broad terms, for flat-plate boundary layers, the lower-frequency end of the power spectrum can be associated with contributions predominantly from large-scale turbulent motion, and the high-frequency end of the spectrum predominantly with contributions from small-scale motion in the inner layer. The characteristic length scales for these two types of motion are, respectively, the boundary layer thickness δ and the wall scale ν/u_τ. Similar relationships are expected to apply for axisymmetric boundary layers.

Further, for cylinders in axial flow, the effects of curvature of the boundary surface can be expected to increase as the thickness of the boundary layer increases in relation to the radius of curvature a. More particularly, effects on the outer layer are expected to increase with δ/a and on the inner layer with δ_i/a, where δ_i is the thickness of the inner layer, typically 30 wall units, so that $\delta_i/a \simeq 30(\nu/u_\tau)/a = 30/a^+$. Transverse curvature can be expected to affect the whole layer significantly only if both parameters are large.

The outer layer in the present experiments is clearly affected by transverse curvature (figure 1). Yet, in spite of

the large variation in δ/a, the wall-pressure spectra show quite close similarity (figure 2) in terms of flat-plate mid-frequency-range scaling – with wall stress τ_w and u_τ/δ as the pressure and frequency scales – and over a similar frequency range to flat-plate boundary layers. There is, however, some small remaining systematic variation with δ/a.

At the same time, the present data also collapse well when scaled in the low-frequency flat-plate form, as $\varphi(\omega)U_0/q^2\delta^*$ as a function of $\omega\delta^*/U_0$. The collapse is good for $\omega\delta^*/U_0$ up to about 0.15, well beyond the limiting flat-plate value of 0.03, and only becomes unsatisfactory towards the upper end of the mid-frequency range ($\omega\delta^*/U_0 \simeq 0.6$). This raises the possibility that transverse curvature extends the boundary-layer dynamics characteristic of the flat-plate low-frequency range to higher frequencies, to an extent which increases with δ/a.

In the present investigation, increases in δ/a, associated with streamwise boundary-layer development, are accompanied by increases in the momentum-thickness Reynolds number of the boundary layer $Re_\theta = U_0\theta/\nu$. Since the wall-shear-stress coefficient $C_f = \tau_w/q$ increases with δ/a at constant Re_θ (Willmarth et al. [8]) but decreases with increasing Re_θ, the two opposing effects result in a C_f value which does not vary significantly over the experimental range. In addition, there is correspondingly little variation of δ/δ^*. Consequently, there is not a large variation in the ratio of frequency scale for the low-frequency range to that for the mid-frequency range, $(\delta/\delta^*)U_0^+$, nor in the ratio of spectral-density scales, $[(U_0^+)^3]/[4(\delta/\delta^*)]$. This may, in part, account for the overlap in frequency range where both low-frequency and mid-frequency scaling appear to be effective. A more general variation of flow parameters is required to define the ranges over which the two forms of scaling might apply; and appeal to experimental results of other investigators does not appear to lead to an unambiguous resolution.

In all the present experiments, a^+ is of the order of 150, and hence δ_i/a is only about 0.2 throughout. The inner layer is therefore expected to be minimally affected by curvature, and to exhibit essentially the same properties as a flat-plate layer at all values of δ/a. The observed spectral similarity in terms of wall parameters in the high-frequency range is consistent with this expectation, but of course gives no indication of possible effects of transverse curvature that might occur when a^+ becomes small and δ_i/a large.

For cylinders at slight angles of yaw ($\beta \leq 1^\circ$), the dimensional spectra on opposite sides of the cylinder are very little different and similar to that for axial flow (figure 4), in spite of dramatic differences in local boundary layer thickness. This implies that these flows have a common scaling, suggesting that the yaw angle has little effect on the distribution of the most effective pressure-producing eddies close to the surface and the thickness of the region of the boundary layer containing them.

At the larger yaw angle of 3°, a major change to the flow has occurred: the boundary layer is now laminar on the windward side of the cylinder, but turbulent on the leeward side. The leeward side exhibits a typical turbulent-layer spectrum very similar to that for the smaller angles of yaw (implying again no great change in the pertinent length scale), while the laminar-layer levels on the windward side are very substantially lower.

At a yaw angle of 9°, the flow has undergone a further major change. Laminar flow again occurs on the windward side, but the pressure spectra on the leeward half are consistent with the occurrence of vortex shedding.

Conclusions

Two main conclusions may be drawn from this study of the wall-pressure fluctuations associated with thick turbulent boundary layers on cylinders in axial and near-axial flow:

(1) Axial-flow wall-pressure spectra for boundary layers with δ/a up to 11.5 appear to scale in a manner consistent with that previously established for planar boundary layers, but the low-frequency range may become more extensive as δ/a increases;

(2) Small angles of yaw, below those at which vortex shedding occurs, produce gross asymmetries in overall boundary-layer thickness, but little change to wall-pressure spectra. This suggests that the thickness of a more central portion of the boundary layer, which is the dominant generator of wall-pressure fluctuations, is relatively insensitive to yaw.

Acknowledgements

The support of the Australian Research Council and Thomson Marconi Sonar Pty. Ltd. is gratefully acknowledged.

References

[1] Bücker, D. and Lueptow, R. M., The boundary layer on a slightly yawed cylinder, *Experiments in Fluids*, **25**, 1998, 487–490.

[2] Bull, M. K., Wall-pressure fluctuations beneath turbulent boundary layers: Some reflections on forty years of research, *J. of Sound and Vib.*, **190**, 1996, 299–315.

[3] Bull, M. K. and Dekkers, W. A., Vortex shedding from cylinders in near axial flow, in *Proceedings of the 10th Australasian Fluid Mechanics Conference*, 1989, 6.41–6.46, 6.41–6.46.

[4] Bull, M. K. and Thomas, A. S. W., High frequency wall-pressure fluctuations in turbulent boundary layers, *Phys. Fluids A*, **19**, 1976, 597–599.

[5] Farabee, T. M. and Casarella, M. J., Spectral features of wall pressure fluctuations beneath turbulent boundary layers, *Phys. Fluids A*, **3**, 1991, 2410–2420.

[6] Schewe, G., On the structure and resolution of wall-pressure fluctuations associated with turbulent boundary-layer flow, *J. Fluid Mech.*, **134**, 1983, 311–328.

[7] Willmarth, W. W., Sharma, L. K. and Inglis, S., The effect of cross flow and isolated roughness elements on the boundary layer and wall pressure fluctuations on circular cylinders, Technical report, The University of Michigan, Dept. of Aerospace Engineering, 1977.

[8] Willmarth, W. W., Winkel, R. E., Sharma, L. K. and Bogar, T. J., Axially symmetric turbulent boundary layers on cylinders: mean velocity profiles and wall pressure fluctuations, *J. Fluid Mech.*, **76**, 1976, 35–64.